ACS APPLIED MATERIALS & INTERFACES

Research Article

www.acsami.org

Inorganic–Organic Thin Implant Coatings Deposited by Lasers

Felix Sima,[†,‡] Patricia M. Davidson,[‡,∥] Joseph Dentzer,[‡] Roger Gadiou,[‡] Emmanuel Pauthe,[§] Olivier Gallet,[§] Ion N. Mihailescu,[†] and Karine Anselme*[,‡]

[†]Lasers Department, National Institute for Lasers, Plasma and Radiation Physics, 409 Atomistilor Street, Magurele, Ilfov, RO-77125, Romania

[‡]Institut de Science des Materiaux de Mulhouse (IS2M), CNRS UMR7361, 15 Rue Jean Starcky, 68057 Mulhouse, France

[§]ERRMECE, Cergy-Pontoise University, 2 Avenue Adolphe Chauvin, 95302 Cergy-Pontoise, France

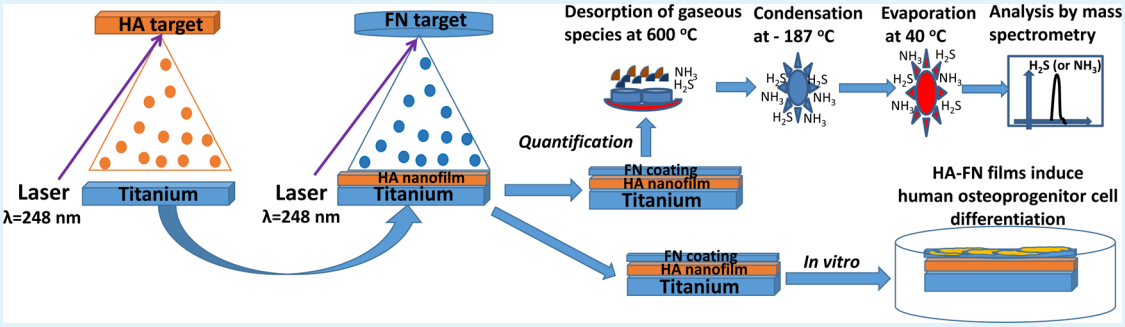

ABSTRACT: The lifetime of bone implants inside the human body is directly related to their osseointegration. Ideally, future materials should be inspired by human tissues and provide the material structure–function relationship from which synthetic advanced biomimetic materials capable of replacing, repairing, or regenerating human tissues can be produced. This work describes the development of biomimetic thin coatings on titanium implants to improve implant osseointegration. The assembly of an inorganic–organic biomimetic structure by UV laser pulses is reported. The structure consists of a hydroxyapatite (HA) film grown onto a titanium substrate by pulsed-laser deposition (PLD) and activated by a top fibronectin (FN) coating deposited by matrix-assisted pulsed laser evaporation (MAPLE). A pulsed KrF* laser source (λ = 248 nm, τ = 25 ns) was employed at fluences of 7 and 0.7J/cm^2 for HA and FN transfer, respectively. Films approximately 1500 and 450 nm thick were obtained for HA and FN, respectively. A new cryogenic temperature-programmed desorption mass spectrometry analysis method was employed to accurately measure the quantity of immobilized protein. We determined that less than 7 μg FN per cm^2 HA surface is adequate to improve adhesion, spreading, and differentiation of osteoprogenitor cells. We believe that the proposed fabrication method opens the door to combining and immobilizing two or more inorganic and organic materials on a solid substrate in a well-defined manner. The flexibility of this method enables the synthesis of new hybrid materials by simply tailoring the irradiation conditions according to the thermo-physical properties of the starting materials.

KEYWORDS: *hydroxyapatite-fibronectin thin films, hybrid materials, laser techniques, cellular studies, protein quantification method*

INTRODUCTION

Recent bioinspired biomaterial strategies have focused on presenting integrin ligands, such as extracellular matrix (ECM) proteins or bioadhesive peptide motifs, on implant surfaces.[1−3] The objective of these strategies is to stimulate cells in the early stage of implantation and accelerate tissue formation around the implant, resulting in subsequent rapid implant integration. Titanium (Ti) is the most commonly used material in implant applications due to its unique properties, including biocompatibility, low density, resistance to corrosion, and ductility. A biomimetic and bioactive thin coating applied on the surface of an implant may be beneficial for bone tissue integration and may even accelerate the entire process. Although many technologies are used to coat titanium and its alloys with calcium phosphates, plasma-spraying is still the technology most frequently used to produce hydroxyapatite (HA) coatings on metallic implants. Comparative studies have demonstrated that pulsed-laser deposition (PLD) could be a promising alternative to plasma-spraying, as PLD overcomes some of the drawbacks of plasma-spraying such as poor thickness control, low adherence, and inhomogeneity.[4] HA coatings obtained by PLD are very dense and crystalline, do not dissolve, and form strong bonds with the bone matrix grown on top.[5] Recently, laser-based transfer of macromolecules has been investigated. However, even at low laser energies, organic materials such as bioadhesive ECM macromolecules would be damaged by such laser-based transfer. To solve this problem, matrix-assisted pulsed laser evaporation (MAPLE) was introduced as an extension of PLD and has been used to grow thin films of polymeric materials with minimal thermal and chemical decomposition

Received: October 28, 2014
Accepted: December 8, 2014
Published: December 8, 2014

as well as control over film thickness, structure, surface morphology, or roughness on substrates for specific applications.[6,7] In contrast to PLD, MAPLE allowed the transport and deposition of delicate, heat-sensitive molecules with minimal degradation. This technique is quickly being developed for single-step organic film fabrication in a double layer[8] or in gradients with variable biodegradable polymeric film composition configurations.[9] Calcium phosphate substrates and, in particular, nanostructured thin films associated with MAPLE-deposited ECM proteins such as fibronectin (FN) are expected to provide a synergistic interface for biomimetic implant applications.[10,11] These biomimetic assemblies are anticipated to provide original properties that may overcome bone tissue engineering issues such as mechanical mismatches between the implant and the natural tissue environment.[12−14]

In this work, we report the two-step fabrication of innovative hybrid biomimetic thin structures solely using laser processing. Deposition onto titanium substrates is achieved by laser vaporization of an inorganic material (HA) and an organic material (FN) in two different laser deposition regimes (PLD and MAPLE, respectively). The metallic substrate ensures mechanical toughness; HA improves biointegration into osseous tissue, and FN accelerates cellular adhesion and will ultimately speed up the formation of new tissue around the implant. The structure and morphology of these hybrid inorganic−organic bilayer structures were characterized. A new method based on temperature-programmed desorption-mass spectrometry (TPD-MS) analysis was used to accurately quantify the very small amount of proteins deposited onto the substrates. The biological efficiency of the proteins after laser transfer was verified by cellular studies.

MATERIALS AND METHODS

Preparation of Titanium Substrates. Disk-shaped grade 4 Ti substrates (1 cm^2, 1 mm thick; Dentaurum GmbH) were mechanically polished and subjected to a double-step etching process. More specifically, initial etching was performed using a solution of 1 M NaOH mixed with 2% v/v H_2O_2 and incubation at 80 °C for 10 min. Subsequently, an acid treatment at 28 °C for 1 h was performed. The substrates were ultrasonically rinsed 3 times for 5 min in distilled water after etching.[15] Before deposition, the substrates were again ultrasonically cleaned in consecutive baths of acetone, ethanol, and deionized water and dried with high purity N_2 gas.

Laser Deposition of Hydroxyapatite Layers. HA powders (Calbiochem (Merck KGaA, 391948)) were pressed and sintered at 500 °C for 6 h to obtain solid compact targets. The targets were irradiated and ablated in a stainless steel chamber using a UV KrF* COMPEX Pro 205 excimer laser source (λ = 248 nm, $\tau \sim 25$ ns). The chamber was initially pumped down to a residual pressure of 10^{-4} Pa. The HA layers were synthesized in a 50 Pa H_2O vapor flux on Ti substrates. Ti collectors were placed at a distance of 4 cm from the HA solid target and heated to 500 °C during deposition. Both the heating and cooling ramps of the substrate were set at 5 °C/min to avoid film deterioration by cracking or peeling. The laser frequency repetition rate was 10 Hz, and the beam was focused to obtain an incident fluence of 7 J cm^{-2} for ablation. During multipulse laser ablation, the target was rotated and translated along 2 orthogonal axes to avoid piercing and to ensure uniform deposition. Twenty thousand pulses were applied for the deposition of one coating. A postdeposition treatment at 500 °C for 6 h in a water vapor-enriched atmosphere completed the first step of the sample preparation procedure in order to restore the H_2O/OH molecules and to improve the crystallinity.[16,17]

Fibronectin Purification and Preparation. FN was purified from human plasma according to a well-established protocol.[18] The purified FN was filtered through a 0.2 μm filter and stored at ±8 °C in 50 mM Tris buffer (pH 7.4) containing 1 mM ethylenediaminetetraacetic acid (EDTA).

Cryogenic FN Aliquot Preparation. Solutions consisting of FN dissolved in saline buffer (TRIS 50 mM pH 7.4, NaCl 150 mM) were gently homogenized and rapidly frozen in a liquid nitrogen-cooled copper container. The container with the frozen target was then mounted on a cryogenic holder inside the reaction chamber and rotated at 10 rpm to avoid local overheating and drilling during multipulse laser irradiation. To protect the protein against laser beam irradiation, the holder was supplied with liquid nitrogen to maintain the target's frozen state during the experiments.

Laser Deposition of FN and BSA Coatings; FN Dropcast Coatings. FN deposition by MAPLE onto HA-coated Ti substrates was carried out according to an established procedure.[19] Bovine serum albumin (BSA) (Santa Cruz) coatings were also deposited onto HA-coated Ti substrates to obtain control structures, as BSA is considered an inert protein with respect to cell adhesion. Protein transfer was conducted at room temperature at a dynamic pressure of 6.5 Pa. The optimal target−substrate separation distance was found to be 3.5 cm. The same pulsed KrF* laser source (λ = 248 nm, $\tau_{fwhm} \approx 25$ ns) operating at 15 Hz was used for MAPLE ablation. Fifteen thousand pulses with a fluence of 0.7J/cm^2 were applied for the deposition of each coating. During MAPLE deposition, the substrates were translated along two orthogonal axes to ensure the synthesis of a uniform film. FN dropcast films on Ti and Ti/HA structures were obtained from solutions consisting of FN dissolved in saline buffer (TRIS 50 mM, pH 7.4, NaCl 150 mM). Drops of 50 μL of FN solution with concentrations of 0.5, 0.25, and 0.125 mg/mL were dried in air on two distinct solid surfaces (Ti and HA-covered Ti).

Surface Morphology Studies by Atomic Force Microscopy. The surface morphology of the obtained structures was investigated by atomic force microscopy (AFM) in tapping mode with a Veeco Multimode AFM powered by a Nanoscope IV controller (Digital Instruments, Santa Barbara, CA). Three samples of each structure were investigated by AFM.

Cryogenic TPD-MS: A New Technique for Mass Quantification of MAPLE-Deposited FN. An important problem in the characterization of organic coatings deposited on inorganic layers is protein quantification. A new method that allows for the quantification of proteins adsorbed on porous materials was recently developed; this method is based on mass spectrometry analysis of low mass gaseous species originating from proteins during temperature-programmed desorption-mass spectrometry (TPD-MS).[20] This method allows the quantification of proteins that exhibit strong interactions with the substrate, as it can be performed after the samples have been washed.[21] Protein amounts varying from 25 to 250 μg were analyzed with good accuracy. However, desorption proceeds over a large temperature range, resulting in very low mass spectrometer signal intensity for very small amounts of proteins and making quantitative analysis difficult. In this study, this method was extended to allow for the accurate quantification of very small amounts of proteins (below 25 μg) on solid substrates. This improvement was achieved by placing a cryogenic trap between the heat treatment chamber and the mass spectrometer to concentrate the evaporating species before analysis. The samples (FN dropcasts and MAPLE-deposited films) were heated to 600 °C at a rate of 2 K/min for complete protein decomposition. All gaseous species formed were condensed on the cryogenic trap (−184 °C). The trap was then heated at 2 K/min from −187 to 40 °C, and evaporating species with low molecular masses were analyzed in vacuum using a quadruple mass spectrometer. For accurate analysis, the spectra were recorded for two gaseous species at m/z = 33−34 and m/z = 15−17 (signals for H_2S and NH_3, respectively), and graphs were plotted against evaporation temperature. For a precise quantification, an experimental calibration of the setup was conducted with previously described FN dropcast films on Ti and HA-covered Ti. Good linearity was found for the two gases on the two surfaces over the range of 6.2−25 μg. One or two samples of each structure were investigated by TPD-MS. For more details, see Table 1.

Surface Wettability. The wettabilities of the different surfaces were obtained from contact angle measurements with 20 μL of pure

Table 1. FN Amounts Deposited by MAPLE on Different Surfaces Estimated by Cryogenic TPD-MS Analysis

number of investigated MAPLE samples	surface	gas	equation	quantity of gas (y = H_2S, NH_3) (μmoles)	estimated quantity (x) (μg)
1	Ti	H_2S	$y = 0.0002x - 0.0002$	0.00132	7.6
1	Ti	NH_3	$y = 0.0071x - 0.0047$	0.04960	7.7
2	Ti	H_2S	$y = 0.0002x - 0.0002$	0.00224	12.2
2	Ti	NH_3	$y = 0.0071x - 0.0047$	0.08600	12.8
1	Ti/HA	H_2S	$y = 0.00009x - 0.0004$	0.00110	7.8
1	Ti/HA	NH_3	$y = 0.0054x - 0.0046$	0.04500	7.5
2	Ti/HA	H_2S	$y = 0.00009x - 0.0004$	0.00180	15.6
2	Ti/HA	NH_3	$y = 0.0054x - 0.0046$	0.07740	13.5

deionized water using a Drop Shape Analysis DSA 10 Mk2 instrument and analysis software. Values were the average of at least five sessile drops from three different samples.

EDS Studies. Samples were investigated under high vacuum in an environmental electronic FEI microscope (Model Quanta 400) before immersion in cellular media as well as after 1 and 3 days of immersion. All elements on 200 μm × 200 μm areas were analyzed from 0 to 11 keV. Three samples of each structure were monitored.

Cell Culture Experiments. Before cell culture experiments, samples were placed in cell culture dishes and sterilized by incubation in a 1% penicillin−streptomycin (Sigma P0781) solution for 1 h followed by two washes in PBS. Experiments were performed with human osteoprogenitor (HOP) cells derived from bone marrow harvested from the sternal bones of cardiac patients during coronary artery bypass graft surgery.[22] Informed consents and ethical committee approvals were granted in all cases. Cells were grown in Iscove's Modified Dulbecco's Medium (IMDM) (Sigma I3390) supplemented with 10% FCS (Sigma F7524), 2 mM L-glutamine (Sigma G7513), and penicillin (100 U/mL)/streptomycin (Sigma P0781) (0.1 mg/mL). Cells were seeded at a density of 17 000 cells/well in a 24-well plate and cultured for up to 21 days to monitor not only cell adhesion but also spreading and surface colonization.

Immunofluorescence Assay for Cell Adhesion Study. HOP cells grown in standard conditions (tissue culture plastic) or in direct contact with the obtained structures were analyzed for actin filaments and vinculin distribution by immunofluorescence microscopy. Cells were fixed with 2% para-formaldehyde for 30 min and permeabilized with 0.2% Triton X-100 for 15 min at room temperature. Cells were then incubated with 0.5% BSA in phosphate buffered saline (PBS) for 1 h at room temperature and stained with TRITC-conjugated Phalloidin (Sigma P-1951) (1:50) for 30 min or with a primary antivinculin antibody (Sigma V-9131) (1:200) followed by a fluorescein isothiocyanate (FITC)-conjugated antimouse immunoglobulin (IgG) antibody (Sigma F-2012) (1:400). Finally, specimens were stained with 100 ng mL^{-1} 4,6-diamidino-2-phenylindole (DAPI) (Sigma, L'Isle d'Abeau, France). Ten fluorescence images per magnification (10×, 20×, and 40×) and per sample were recorded with an Olympus fluorescence microscope (BX-51). Three samples of each structure were monitored in parallel at various time intervals (1, 3, or 7 days).

Immunofluorescence Assay of Fibronectin Secretion. Detection of secreted FN was performed by immunofluorescent staining. Samples were immersed in 3% nonfat milk in PBS buffer for 30 min at room temperature. After saturation, samples were incubated for 1 h in rabbit antihuman plasma fibronectin polyclonal antibody (Sigma F-3648) (1:100 in saturation buffer), rinsed three times with the same buffer, and incubated again for 1 h at room temperature with FITC-conjugated goat antirabbit IgG (Sigma F-0382) (1:100). Finally, samples were washed 3 times with saturation buffer. Control experiments with primary antibody only were performed. Fluorescence images were recorded with an Olympus BX-51 fluorescence microscope. Three samples of each structure were monitored in parallel at various time intervals (1, 3, or 7 days).

SEM Analysis. Cells were seeded on samples at a density of 17 000 cells/well in a 24-well plate and analyzed after 7 days of incubation. Samples were washed at room temperature with PBS (3 times × 5 min). The cells were fixed with 2% para-formaldehyde and 4% glutaraldehyde in NaK_2PO_4 for 30 min at room temperature. After a 2 h washing in NaK_2PO_4 (17%), the cells were dehydrated in ethanol baths of increasing concentration, 50%, 70%, 80%, 95%, and 100% (with 2−3 baths of 5 min for each concentration), followed by dehydration in baths of 50% hexamethyldisilazane (HMDS) in ethanol and 100% HMDS for 10 min each. The samples were then left to dry out completely. Next, specimens were analyzed under high vacuum in an environmental electronic FEI microscope (Model Quanta 400). Three samples of each structure were monitored.

MTT Proliferation Assay. The samples were analyzed at 1, 3, 7, 14, and 21 days. After cell seeding and culture, samples were transferred to a new 24-well plate. One mL of MTT (Thiazolyl Blue Tetrazolium Blue, Sigma M5655), 10× diluted in warm PBS (37 °C), was added on each sample. The plates were incubated at 37 °C for 3 h, after which the supernatant was removed. The cells were lysed in 0.1 M HCl in isopropanol and homogenized for 10 min. The optical density at 570 nm, which is proportional to the number of viable cells on the surfaces, was recorded. Three measurements for each sample were carried out.

ALP Enzymatic Activity Assay. The samples were analyzed at 14 and 21 days. After cell seeding, samples were transferred to a new 24-well plate. After washing with warm PBS (37 °C), we added 150 μL of Triton-X-100 (0.5% in H_2O) and 150 μL of substrate solution (pNPP) to each well and incubated the plate at 37 °C for 30 min. We then added 150 μL of blocking solution and measured the absorption at 405 nm. The substrate solution consisted of 20 mM *p*-nitrophenyl phosphate, 100 mM diethanolamine (98%), and 10 mM $MgCl_2$ at a pH of 9.5, while the blocking solution consisted of 0.1 M EDTA and 2 M NaOH. Three measurements for each sample were taken.

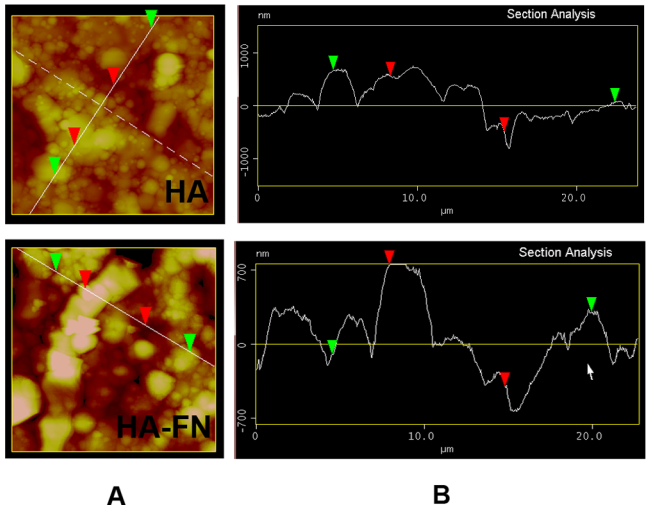

Figure 1. Representative AFM images of a pulsed laser-deposited HA film on a Ti substrate (top) and of MAPLE-deposited FN on Ti/HA structures (bottom). Granular, compact surface morphologies with micronic features were observed for both structures (A). Line profiles (B) corresponding to AFM data from (A). From these profiles, step heights of approximately 697 and of 1149 nm between the highest and lowest regions can be inferred for the HA and HA/FN coatings, respectively.

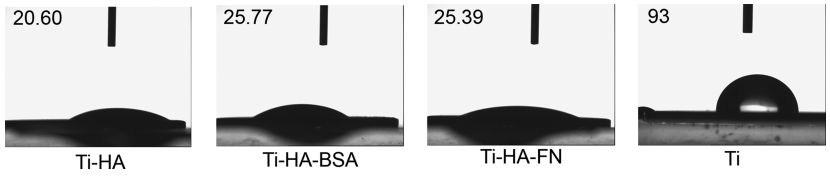

Figure 2. Selected images and contact angles (as recorded by software) for (left to right): Ti/HA, Ti/HA/BSA, Ti/HA/FN ,and Ti. Three samples of each structure were measured.

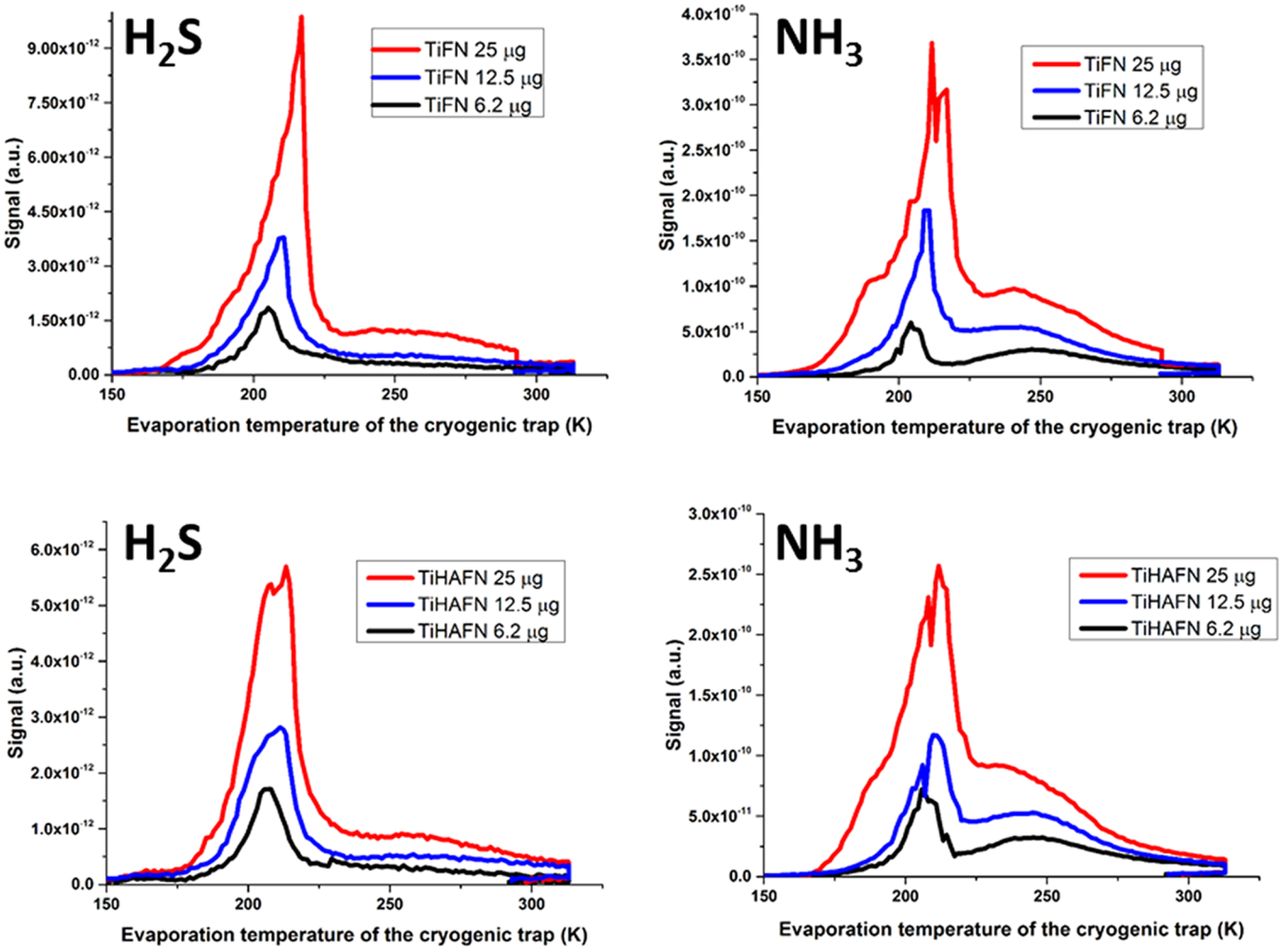

Figure 3. Evaporation profiles of trapped species from FN dropcast coatings deposited onto Ti (top) and Ti/HA structures (bottom). The profiles were recorded for two gas species: H_2S (left) and NH_3 (right).

Statistical Analysis. All statistical analyses were performed using GraphPad Prism 4 Software. The student's *t* test was used to determine statistical significance between samples (differences: $*p < 0.05$). Data are presented as the mean ± s.e.m.

RESULTS

Physico-Chemical Characterization of Coatings. AFM images and profiles of HA films deposited by PLD onto Ti (Ti/HA) as well as FN coatings transferred by MAPLE onto Ti/HA structures are presented in Figure 1.

A granular surface morphology was observed with micro- and nanocavities characterized by peak-to-valley clusters with Rz values of 0.7 ± 0.1 μm for HA and of 1.1 ± 0.1 μm for HA/FN coatings. Rms and Ra values are similar to submicrometric values of 373 ± 10 and 207 ± 70 nm for the HA and HA/FN coatings, respectively. Surface roughness was slightly increased by the addition of the protein layer. Irregular structures such as fibrils and aggregates were visible on surfaces. We found that salts were also transferred to the substrate along with FN.

Hydrophilic character was observed for all deposited structures. Ti surfaces are hydrophobic, as characterized by a contact angle of 93 ± 3°. A significant decrease in the contact angle was obtained in the case of Ti/HA (20 ± 5), Ti/HA/BSA (25 ± 5), and Ti/HA/FN (25 ± 5), as shown in Figure 2.

EDS studies confirmed a systematic change in the Ca/P ratio of the coatings after interacting with cells and cellular media depending on the protein deposited on top of the HA layer. For HA, the Ca/P ratio varies from an initial 1.51 to 1.27 during the first day of cell culture, followed by an increase at day 3 (1.5). This behavior is different for HA/BSA and HA/FN: in the first day of culture, the Ca/P ratio decreases to values of 1.2 and 1.15 for HA/BSA and HA/FN, respectively,

dx.doi.org/10.1021/am507153n | ACS Appl. Mater. Interfaces 2015, 7, 911−920

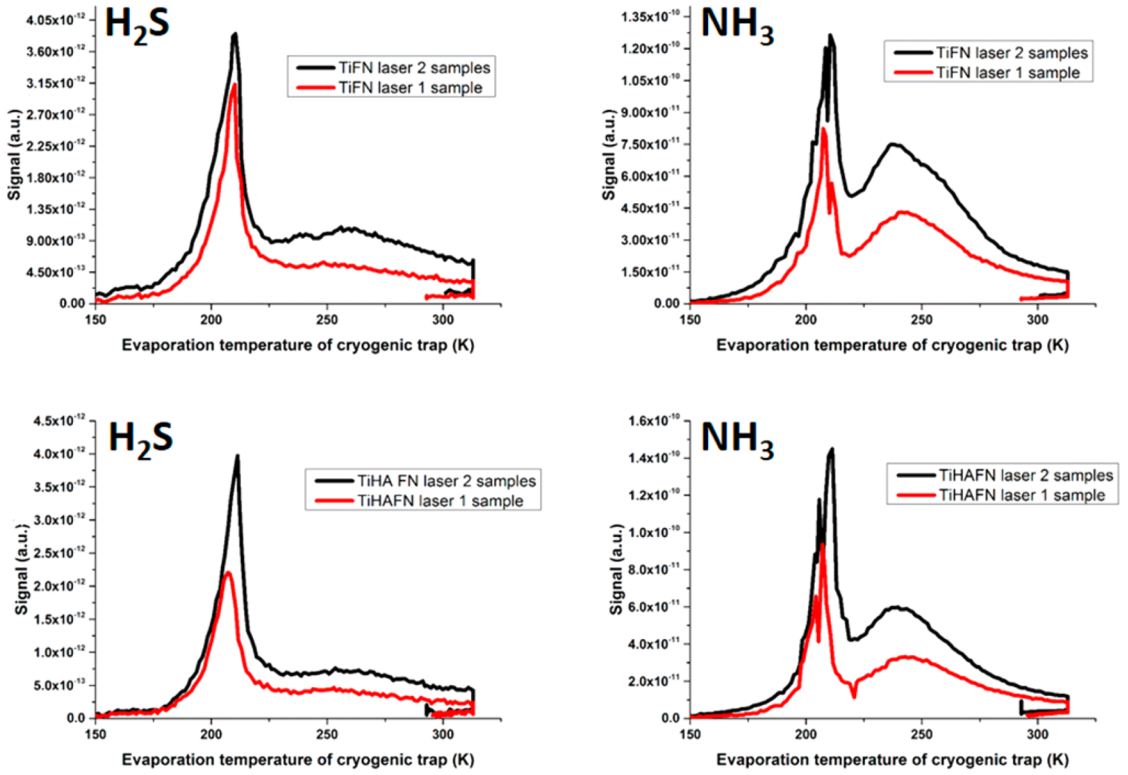

Figure 4. Evaporation profiles of trapped species from MAPLE deposited coatings onto Ti (top) and Ti/HA structures (bottom), respectively. Profiles were recorded for two species of gases: H_2S (left) and NH_3 (right).

and then increases at day 3 to 1.31 and 1.25 for HA/BSA and HA/FN, respectively.

Quantification of MAPLE-Deposited FN. Figure 3 shows the recorded profiles (H_2S and NH_3 signal vs trap temperature) of FN dropcast coatings deposited on Ti (TiFN) and Ti/HA (TiHAFN) used for the calibration of cryogenic TPD-MS. The profiles are similar in shape with an evaporation peak at 208 K. The signal intensity and peak width are proportional to the quantity of protein from which the two gases were generated.

From the calibration experiments, we can measure the quantities of laser-transferred FN on Ti and Ti/HA substrates. We used either one or two samples to estimate the accuracy of the technique; the values obtained are shown in Table 1. We measured approximately 7.8 μg of FN deposited onto 1.13 cm^2 round HA structures (results obtained by H_2S monitoring). The values obtained for two samples were not exactly twice the amount obtained for one sample; however, the errors are within margin of errors of the methods, both for MAPLE experiments and TPD-MS analyses.

Figure 4 shows the recorded profiles of species collected from FN coatings deposited by MAPLE obtained by laser evaporation. These profiles are similar to those of dropcast coatings, peaking at ~208 K. The signal intensity and broadening are proportional to the FN quantity for both gases and the investigated surface area.

Cellular Experiments. Normal distributions of cytoskeleton filaments and optimal cell density were observed after 1, 3, and 7 days. Figure 5 shows the fluorescence microscopy single channel and merged images after staining of actin filaments, vinculin focal points, and nuclei. After 1 day, cells grown on FN coated structures interact more intimately with the substrate than cells on Ti/HA (data not shown) and Ti/HA/BSA. Cells grown on Ti/HA/FN surfaces exhibit more clearly visible focal adhesion points (see arrow in Figure 5E), better cell spreading, and more elongated cytoplasmic protrusions. Generally, focal adhesion points are difficult to visualize on porous-like materials such as HA coatings, as focal adhesion points are approximately 10−15 nm in size. After 7 days, cells on FN tended to cluster (Figure 5H), while cells on BSA coatings remained dispersed (Figure 5D). The cells remain viable and proliferate on all surfaces investigated.

SEM images of cells grown on Ti/HA, Ti/HA/BSA, and Ti/HA/FN for 7 days are given in Figure 6. For completeness, we show a SEM image of a raw HA film grown by PLD on a Ti substrate maintained in cell culture media for 7 days (bottom right). This image depicts a uniform and homogeneous material surface, confirming film stability under liquid media. Close contact of cells with all surfaces is clear, with abundant filopodia on FN-covered structures. Visible porous, matrix-like structures were observed in samples with adsorbed protein layers.

We checked if laser-transferred FN was still visible on the biomaterial surface after 1 day of culture. Interestingly, we observed a well-organized network of cells which could be the result of secreted cellular FN (cFN) or/and plasmatic MAPLE-deposited FN (pFN) that has been remodeled by the cells (Figure 7). cFN originates from around the nucleus (day 1) and extends to a complex dense network (day 7). This trend was observed in all Ti/HA/FN samples. The cells grown on Ti/HA and Ti/HA/BSA surfaces produced cFN, but these networks were not as well developed after 1 day (Figure 8) or subsequent days (data not shown), especially for cells grown on Ti/HA/BSA.

Figure 9A presents the MTT quantification of viable cells on Ti/HA (HA), Ti/HA/FN (HA/FN), and Ti/HA/BSA (HA/BSA)

dx.doi.org/10.1021/am507153n | ACS Appl. Mater. Interfaces 2015, 7, 911−920

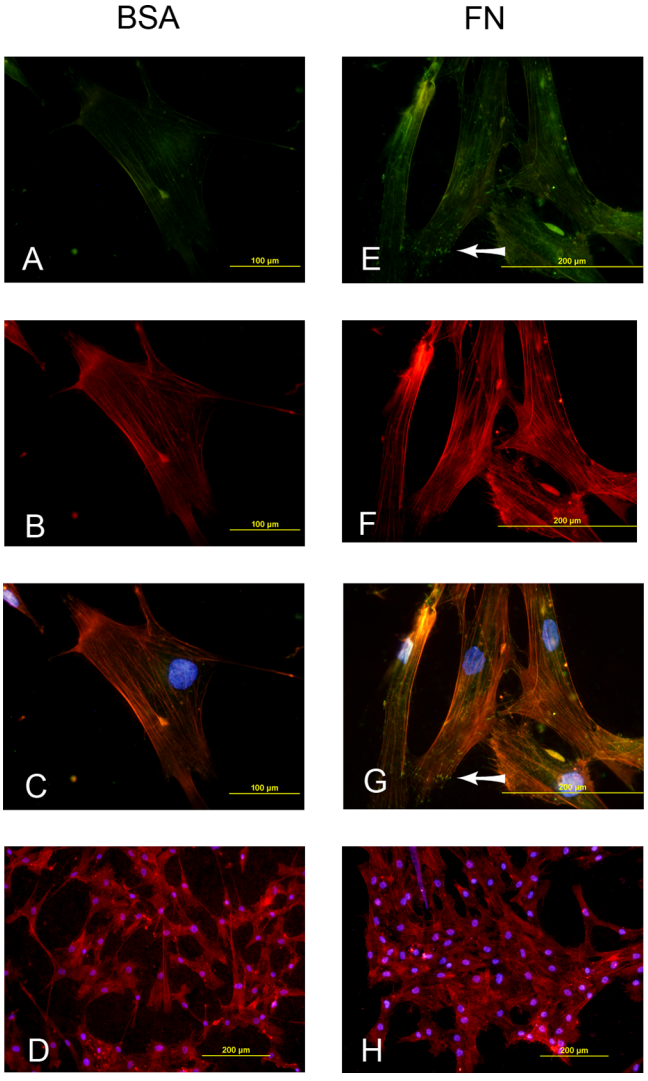

Figure 5. Vinculin (A, E) and actin (B, F) staining of HOP cells after 1 day of cultivation on Ti/HA/BSA (A, B, C) and Ti/HA/FN (E, F, G) selected samples. Superposition of actin, vinculin, and DAPI staining of HOP cells grown on Ti/HA/BSA (C) and Ti/HA/FN (G). Actin and DAPI staining of HOP cells after 7 days of cultivation on Ti/HA/BSA (D) and Ti/HA/FN (H). Three samples of each structure were monitored in parallel.

samples at 1, 3, 7, 14, and 21 days. For a meaningful quantification, the results were normalized to the activity of cells cultured on bare Ti. It should be noted that Ti was not considered a real reference but rather a control material in our study. One clearly observes different cellular behaviors after the first day, with cells adhering faster to HA coatings. Also, on the first day, either BSA or FN coatings appear to have an inhibitory effect on cell proliferation compared to HA. For all coatings, the number of cells is more or less constant until day 7, after which the number of cells increases. A relative decline in the number of cells is observed between days 14 and 21.

The alkaline phosphatase (ALP) activity of HOP cells on coatings was then investigated. Figure 9B depicts the production of ALP normalized to the number of cells obtained using the MTT activity. It can be observed that FN induces a higher alkaline phosphatase activity at day 21 in comparison with the cells grown on HA or HA/BSA structures. This result confirms that less than 7 μg of FN per cm^2 deposited by MAPLE on HA

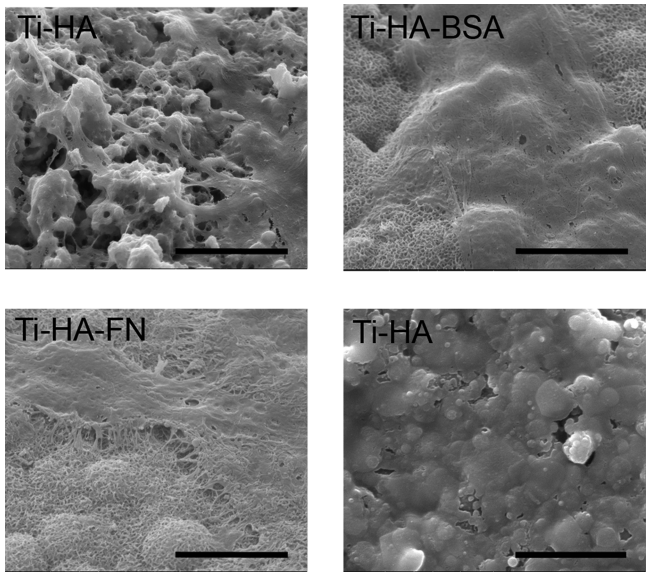

Figure 6. SEM images of cells grown for 7 days on Ti/HA, Ti/HA/BSA, and Ti/HA/FN. Bottom right: image of Ti/HA immersed in cell culture medium for 7 days. Three samples of each structure were monitored. Scale bars are 10 μm.

coatings can improve HOP differentiation over HA coatings alone.

DISCUSSION

During the osseointegration process, two factors play important roles: primary and secondary mechanical stability. Secondary stability pertains to biological stability after bone remodeling and requires that the implant promotes osteogenic cell differentiation. Fibronectin has been proposed to improve biomaterials designed for bone reconstruction as well as enhance osseointegration[23] and has been shown to play an important role in wound healing and tissue repair.[24] It is anticipated that coating dental implants with FN could improve the success rate for tissue regeneration.[25] FN immobilized on HA ceramic surfaces by coprecipitation in a supersaturated calcium phosphate solution enhanced the spreading and osteogenic differentiation of human MSCs *in vitro*.[26] FN preadsorption on smooth and rough HA substrates was found to increase the number of attached osteoblasts by 40% and 62% and increased osteoblast attachment strength by 165% and 73%, respectively.[27] Our results confirmed these observations.

Many studies have been performed using PLD to obtain HA coatings with superior mechanical, physical−chemical, and biological properties. It was found that laser fluence is an important factor for developing HA coatings with improved biological properties.[17] The method was upgraded by developing novel, more stable lasers and beam homogenizers that allow for better control of film thickness and stoichiometry. In our PLD experiments, we optimized deposition parameters from mechanical and biological standpoints.[17,28] The optimized laser parameters were shown to grow very thin coatings less than 1.5 μm in thickness with improved adhesion properties. This ability prevents film cracking or peeling, which usually appear when the film is thicker, as dissolution in thicker films is harder to control. Rough HA surfaces obtained by PLD were found to be biocompatible and to improve cellular adhesion, proliferation, and most importantly differentiation.[29]

dx.doi.org/10.1021/am507153n | ACS Appl. Mater. Interfaces 2015, 7, 911−920

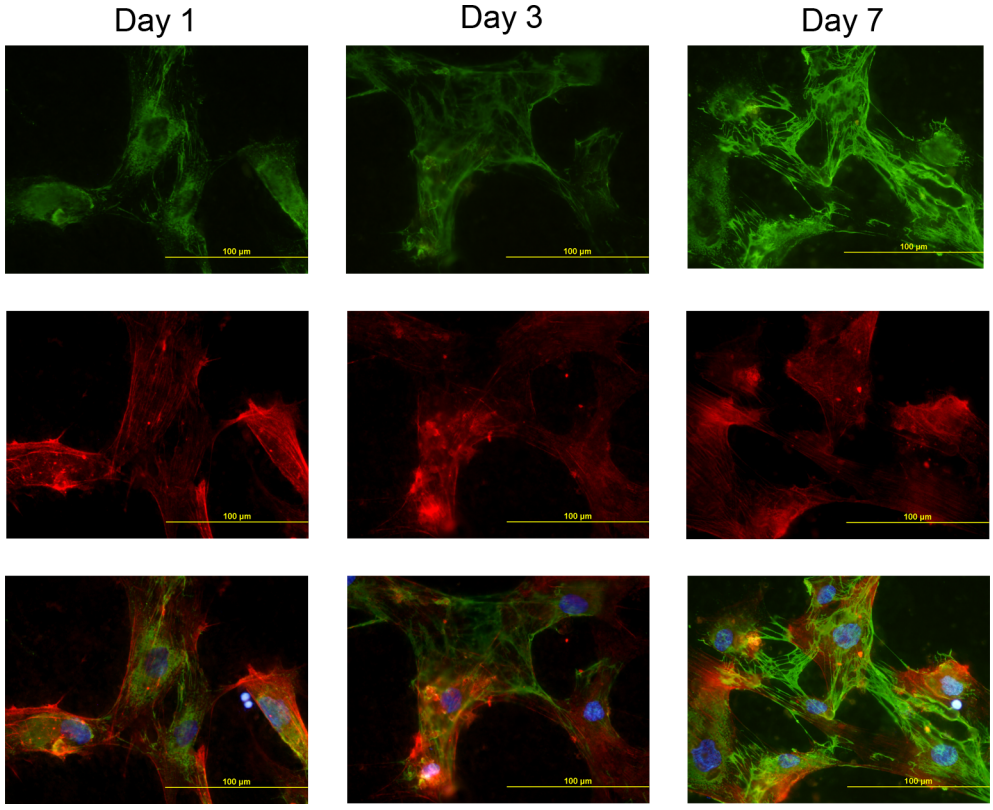

Figure 7. Staining of FN (green) and actin filaments (red) of cells grown on Ti/HA/FN structures at 1, 3, and 7 days. The cells were fixed, permeabilized, and stained for actin with TRITC conjugated phalloidin (red) and for FN with anti-FN FITC conjugated antibody (green). The nuclei were stained by DAPI (blue). Images of actin, nuclei, and FN are superimposed in the last row. Three samples of each structure were monitored in parallel.

These films are polycrystalline, very adherent to substrates, resistant, and active in simulated body fluids and cellular media.[30]

We hypothesize that the combination of a thin layer of HA and a very small amount of FN deposited as an interface layer between an orthopedic device and the host tissue could overcome well-known implant problems. The affinity of FN to HA is due to the strong bonding between FN and Ca ions.[10] Moreover, using both nano- and macro-HA features specific to the PLD process, we expect a FN-HA synergistic effect, as adhesion of osteoblast-like cells is improved by FN adsorption on nanoscale HA.[31] This expectation is the reason we applied a second laser deposition step by MAPLE to obtain a thin coating of FN and to improve cell attachment. Preliminary studies permitted us to optimize the thickness of the HA layer to approximately 1−1.5 μm[29,32] and to 450 nm for FN coating.[19] A granular surface morphology was observed by AFM for all laser-deposited coatings with uniformly distributed micro- and nanocavities. The surface roughness was slightly increased by the addition of the protein layer. Salts were also transferred to the substrate together with FN. However, these salts did not influence the coating's biocompatibility, and we believe that these salts could be involved in protein stabilization on the HA surface.

Our studies revealed hydrophilic characters for all of the deposited structures. The surface wettability (hydrophilic or hydrophobic character) contributes to cellular adhesion.[33] Studies with fibroblasts demonstrated that cells are well-spread and exhibit more extended actin filaments when grown on hydrophilic surfaces.[34,35] The synergistic effect of HA/FN biphase assembly on cellular adhesion could be enhanced by the hydrophilic behavior of the coating. However, because the hydrophilicity is similar for all structures obtained after laser deposition, this parameter should not be a key factor in parametric studies of the performance of these biomaterials. Additionally, the influence of the hydrophilic character of the surface is surely less than the influence of integrin-FN affinity.[36] A synergy between high surface energy, chemistry, and topography at both micron and submicron scale has been shown to promote osteoblast response and may lead to innovative biomaterial designs to improve host tissue response.[37]

We propose that the proteins deposited on the HA coating may play the role of HA nucleator in the cellular medium, leading to the formation of a mimetic biogenic environment.[12] Our EDS studies effectively confirmed systematic changes in the Ca/P ratio of the coatings upon interactions with cells and cellular media only on surfaces with proteins (FN or BSA) deposited on the HA layer. The matrix-like structures observed on samples with adsorbed protein layers could eventually become associated with precipitated ions from the culture medium, resulting in a more dynamic exchange with the active surface. Indeed, in other studies, small amounts of FN were found to promote calcium deposition in standard medium after 21 days in cell culture as well as further mesenchymal stem cell growth and differentiation in osteoblasts.[38]

In a previous study, the preservation of FN integrity and functionality after laser transfer on silicon wafers was demonstrated thanks to Fourier transform infrared spectrometry (FTIR), resulting in superior attachment of osteoprogenitor cells grown on FN coatings.[19] In the present study, we have focused on the

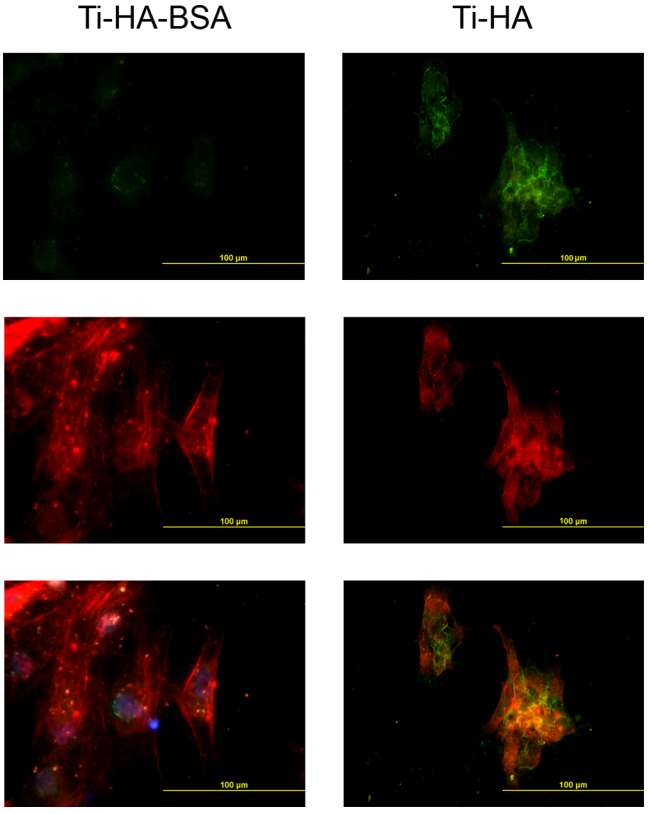

Figure 8. Staining of FN (green) and actin filaments (red) of cells grown on Ti/HA/BSA and Ti/HA structures at 1 day. The cells were fixed, permeabilized, and stained for actin with TRITC conjugated phalloidin (red) and for FN with anti-FN FITC conjugated antibody (green). The nuclei were stained by DAPI (blue). Images of actin, nuclei, and FN are superimposed in the last row. Three samples of each structure were monitored in parallel.

synergistic effect of HA/FN grown layers on cellular activity by monitoring the behavior of osteoprogenitor cells at different times (1, 3, 7, 14, and 21 days). Ti/HA/FN assemblies were analyzed in comparison with control structures Ti, Ti/HA, and Ti/HA/BSA. BSA or FN coatings appeared to have an inhibitory effect on cell attachment, likely due to an initial perturbation of adhesive protein adsorption from serum.[39] After 1 day, cells grown on FN-coated structures more intimately interacted with the substrate than cells grown on Ti/HA/BSA. Additionally, cells grown on FN exhibited focal adhesion points and more elongated cytoplasmic protrusions, as previously described.[40,41]

After just 3 days of culture, a well-organized FN network was observed on Ti/HA/FN samples. This network could be the result of secreted cellular FN or/and plasmatic MAPLE-deposited FN remodeled by the cells. It has been shown that osteoblast-like cells deposit well-organized cFN as a network on the top of various rough Ti surfaces precoated with FN.[42] The authors observed that secreted FN was present mostly on the peaks of the surface features. Low amounts (60 μg/mL per well) of FN precoated surfaces were found to initiate the cellular FN assembly process via the accumulation of high density fibrils. *In vivo* studies demonstrated that coating the implant with pFN induced faster osseointegration due to the recruitment of a larger number of cFN and osteoprogenitor cells close to the implant surface via the preferential chemotactic activity of pFN.[23]

In our investigations, the cells proliferated on all tested surfaces from day 1 to 14, but a relative decline was observed between days 14 and 21 (see Figure 9A). In the case of osteoprogenitor cells, this behavior was quite systematic and has been observed in other studies, which report improved osteogenesis on hydroxyapatite[43] and a reversed balance between proliferation and differentiation when using Dex-induced differentiation medium.[44] Cell proliferation stopped after 21 days even on HA coatings, likely due to increased differentiation.[45] It was recently shown that osteoblast attachment and differentiation are enhanced on HA surfaces with increased submicro- and microscale complexity.[46] Other studies demonstrated that bioactive nano-HA coatings on Ti implants with micronscale concavities are promising environments for stem cell niches in bone tissue engineering and regenerative medicine.[47]

Our results suggest that osteogenic differentiation of osteoprogenitor cells (Figure 9B) is potentially influenced by the synergistic interaction of small amounts of laser-deposited FN with calcium-based compounds. These hybrid materials effectively mimic not only the microenvironment but also the interactions that occur in the natural ECM as well, as these materials contain mineral-binding domains that have been demonstrated to promote cell proliferation and differentiation.[48] The questions of which molecules should be incorporated into which coating and using what method as well as the dosage and optimal delivery time should be addressed for specific biological processes and applications such as

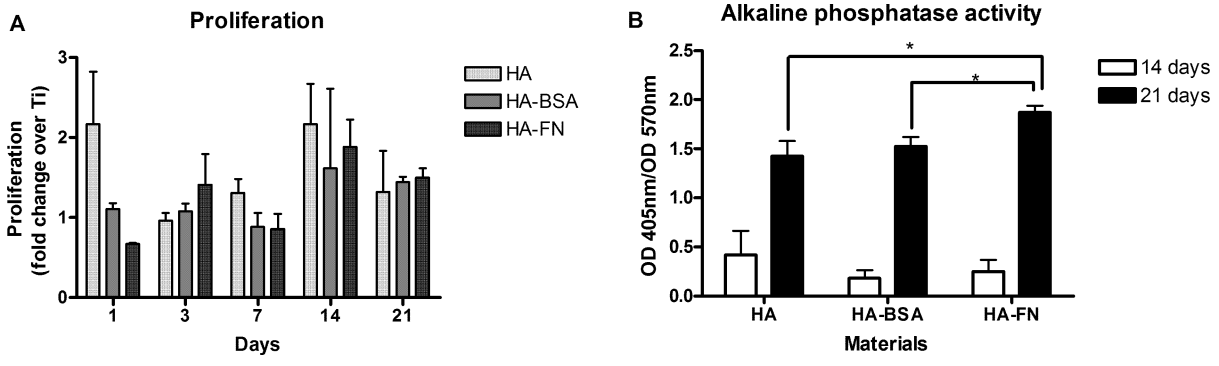

Figure 9. Proliferation of HOP cells over 21 days (A) and alkaline phosphatase activity (ALP/MTT ratio) at days 14 and 21 (B) on HA, HA/BSA, and HA/FN structures. Three samples of each structure were monitored in parallel. Three measurements for each sample were taken. Mean, $n = 3$ triplicates, $^*p < 0.05$.

dx.doi.org/10.1021/am507153n | ACS Appl. Mater. Interfaces 2015, 7, 911−920

orthopedics or dentistry. We believe that modified bioactive HA surfaces with submicron and microfeatures in combination with well-chosen organic molecules could lead to new implant designs with improved functionality and biological efficiency. Additionally, stable FN micropatterned structures could provide precise control of cellular organization.[49] A 3D submicron HA configuration associated with a controlled FN coating could promote and accelerate the osseointegration process, creating a strong interface. Bone-bonding will thus rely upon submicron features, and interfacial stability under loading will result from micronscale characteristics.[50]

CONCLUSIONS

A biomimetic-like-implant structure was developed solely using advanced pulsed laser methods. A biphasic biomimetic "sandwich" system composed of hydroxyapatite particles associated with small amounts of fibronectin was fabricated on a titanium substrate. The films were compact with microgranular features within the volume investigated and exhibited a rather rough surface with larger particulates on the top. Less than 10 μg per cm^2 of FN on the HA surface was successfully quantified using a new cryogenic TPD-MS analysis method. Cellular studies demonstrated that a HA layer on Ti discs coated with ~7 μg per cm^2 of FN encourages adhesion, spreading, and finally differentiation of HOP cells. We hypothesize that the FN layer may reduce the duration of the initial mechanical biointegrating phase while the underlying HA coating should improve actual implant integration within the organism. The proposed fabrication method opens the door for one to combine and immobilize two or more inorganic and organic materials on a solid substrate in a well-defined manner. The method's flexibility allows for the synthesis of new hybrid materials by simply tailoring the irradiation conditions according to the thermo-physical properties of the starting materials.

AUTHOR INFORMATION

Corresponding Author

*E-mail: karine.anselme@uha.fr.

Present Address

[‖]Weill Institute for Cell and Molecular Biology, Cornell University, Ithaca, New York 14853.

Author Contributions

The manuscript was written through contributions from all authors. All authors have approved the final version of the manuscript.

Notes

The authors declare no competing financial interest.

ACKNOWLEDGMENTS

The bilateral contract ANR-UEFISCDI n. 19 RO-FR Biocoat_By_Laser (2013-2016) is gratefully acknowledged. F.S. gratefully acknowledges the support of the PN-II-RU-PD-2011-3-0147 (101/2012) contract.

REFERENCES

(1) Murphy, M. B.; Hartgerink, J. D.; Goepferich, A.; Mikos, A. G. Synthesis and *in Vitro* Hydroxyapatite Binding of Peptides Conjugated to Calcium-Binding Moieties. *Biomacromolecules* **2007**, *8*, 2237−2243.

(2) Badylak, S. F.; Freytes, D. O.; Gilbert, T. W. Extracellular Matrix as a Biological Scaffold Material: Structure and Function. *Acta Biomater.* **2009**, *5*, 1−13.

(3) Mas-Moruno, C.; Fraioli, R.; Albericio, F.; Manero, J. M. A.; Gil, F. J. Novel Peptide-Based Platform for the Dual Presentation of Biologically Active Peptide Motifs on Biomaterials. *ACS Appl. Mater. Interfaces* **2014**, *6*, 6525−6536.

(4) Garcia-Sanz, F.; Mayor, M.; Arias, J.; Pou, J.; Leon, B.; Perez-Amor, M. Hydroxyapatite Coatings: A Comparative Study between Plasma-Spray and Pulsed Laser Deposition Techniques. *J. Mater. Sci.: Mater. Med.* **1997**, *8*, 861−865.

(5) Cleries, L.; Fernández-Pradas, J.; Morenza, J. Bone Growth on and Resorption of Calcium Phosphate Coatings Obtained by Pulsed Laser Deposition. *J. Biomed. Mater. Res.* **2000**, *49*, 43−52.

(6) Piqué, A.; Chrisey, D.; Spargo, B.; Bucaro, M.; Vachet, R.; Callahan, J.; McGill, R.; Leonhardt, D.; Mlsna, T. Use of Matrix Assisted Pulsed Laser Evaporation (MAPLE) for the Growth of Organic Thin Films. *MRS Online Proc. Libr.*, **1998**, *526*, 421; DOI: 10.1557/PROC-526-421.

(7) Shepard, K. B.; Priestley, R. D. MAPLE Deposition of Macromolecules. *Macromol. Chem. Phys.* **2013**, *214*, 862−872.

(8) Caricato, A.; Cesaria, M.; Gigli, G.; Loiudice, A.; Luches, A.; Martino, M.; Resta, V.; Rizzo, A.; Taurino, A. Poly-(3-hexylthiophene)/[6,6]-Phenyl-C61-butyric-acid-methyl-ester Bilayer Deposition by Matrix-Assisted Pulsed Laser Evaporation for Organic Photovoltaic Applications. *Appl. Phys. Lett.* **2012**, *100*, 073306.

(9) Sima, F.; Axente, E.; Sima, L.; Tuyel, U.; Eroglu, M.; Serban, N.; Ristoscu, C.; Petrescu, S.; Oner, E. T.; Mihailescu, I. Combinatorial Matrix-Assisted Pulsed Laser Evaporation: Single-Step Synthesis of Biopolymer Compositional Gradient Thin Film Assemblies. *Appl. Phys. Lett.* **2012**, *101*, 233705.

(10) Gailit, J.; Ruoslahti, E. Regulation of the Fibronectin Receptor Affinity by Divalent Cations. *J. Biol. Chem.* **1988**, *263*, 12927−12932.

(11) Pellenc, D.; Berry, H.; Gallet, O. Adsorption-Induced Fibronectin Aggregation and Fibrillogenesis. *J. Colloid Interface Sci.* **2006**, *298*, 132−144.

(12) Gajjeraman, S.; He, G.; Narayanan, K.; George, A. Biological Assemblies Provide Novel Templates for the Synthesis of Biocomposites and Facilitate Cell Adhesion. *Adv. Funct. Mater.* **2008**, *18*, 3972−3980.

(13) Sima, F.; Mihailescu, I. N. Biomimetic Assemblies by Matrix-Assisted Pulsed Laser Evaporation. In *Laser Technology in Biomimetics*; Springer: Heidelberg, 2013; pp 111−141.

(14) Motoc, M.; Axente, E.; Popescu, C.; Sima, L.; Petrescu, S.; Mihailescu, I.; Gyorgy, E. Active Protein and Calcium Hydroxyapatite Bilayers Grown by Laser Techniques for Therapeutic Applications. *J. Biomed. Mater. Res., Part A* **2013**, *101*, 2706−2711.

(15) Giordano, C.; Sandrini, E.; Del Curto, B.; Signorelli, E.; Rondelli, G.; Di Silvio, L. Titanium for Osteointegration: Comparison Between a Novel Biomimetic Treatment and Commercially Exploited Surfaces. *J. Appl. Biomater. Biomech.* **2004**, *2*, 35−44.

(16) Mihailescu, I.; Torricelli, P.; Bigi, A.; Mayer, I.; Iliescu, M.; Werckmann, J.; Socol, G.; Miroiu, F.; Cuisinier, F.; Elkaim, R. Calcium Phosphate Thin Films Synthesized by Pulsed Laser Deposition: Physico-Chemical Characterization and *in Vitro* Cell Response. *Appl. Surf. Sci.* **2005**, *248*, 344−348.

(17) Ball, M.; Downes, S.; Scotchford, C.; Antonov, E.; Bagratashvili, V.; Popov, V.; Lo, W.-J.; Grant, D.; Howdle, S. Osteoblast Growth on Titanium Foils Coated with Hydroxyapatite by Pulsed Laser Ablation. *Biomaterials* **2001**, *22*, 337−347.

(18) Poulouin, L.; Gallet, O.; Rouahi, M.; Imhoff, J.-M. Plasma Fibronectin: Three Steps to Purification and Stability. *Protein Expression Purif.* **1999**, *17*, 146−152.

(19) Sima, F.; Davidson, P.; Pauthe, E.; Sima, L.; Gallet, O.; Mihailescu, I.; Anselme, K. Fibronectin Layers by Matrix-Assisted Pulsed Laser Evaporation from Saline Buffer-Based Cryogenic Targets. *Acta Biomater.* **2011**, *7*, 3780−3788.

(20) Gadiou, R.; Dos Santos, E.; Vijayaraj, M.; Anselme, K.; Dentzer, J.; Soares, G.; Vix-Guterl, C. Temperature-Programmed Desorption as a Tool for Quantification of Protein Adsorption Capacity in Micro-and Nanoporous Materials. *Colloids Surf., B* **2009**, *73*, 168−174.

(21) Vijayaraj, M.; Gadiou, R.; Anselme, K.; Ghimbeu, C.; Vix-Guterl, C.; Orikasa, H.; Kyotani, T.; Ittisanronnachai, S. The Influence of Surface Chemistry and Pore Size on the Adsorption of Proteins on Nanostructured Carbon Materials. *Adv. Funct. Mater.* **2010**, *20*, 2489−2499.
(22) Anselme, K.; Broux, O.; Noel, B.; Bouxin, B.; Bascoulergue, G.; Dudermel, A. F.; Bianchi, F.; Jeanfils, J.; Hardouin, P. *In Vitro* Control of Human Bone Marrow Stromal Cells for Bone Tissue Engineering. *Tissue Eng.* **2002**, *8*, 941−53.
(23) J Jimbo, R.; Sawase, T.; Shibata, Y.; Hirata, K.; Hishikawa, Y.; Tanaka, Y.; Bessho, K.; Ikeda, T.; Atsuta, M. Enhanced Osseointegration by the Chemotactic Activity of Plasma Fibronectin for Cellular Fibronectin Positive Cells. *Biomaterials* **2007**, *28*, 3469−3477.
(24) Thibault, M. M.; Hoemann, C. D.; Buschmann, M. D. Fibronectin, Vitronectin, and Collagen I Induce Chemotaxis and Haptotaxis of Human and Rabbit Mesenchymal Stem Cells in a Standardized Transmembrane Assay. *Stem Cells Dev.* **2007**, *16*, 489−502.
(25) Ogura, N.; Kawada, M.; Chang, W.-J.; Zhang, Q.; Lee, S.-Y.; Kondoh, T.; Abiko, Y. Differentiation of the Human Mesenchymal Stem Cells Derived from Bone Marrow and Enhancement of Cell Attachment by Fibronectin. *J. Oral Sci.* **2004**, *46*, 207−213.
(26) Yu, S.; Atsuo, I.; Tomonori, M.; Ayako, O.; Gaku, T.; Tazuko, S.; Atsushi, Y.; Eiji, U.; Tadao, O. Fibronectin−Calcium Phosphate Composite Layer on Hydroxyapatite to Enhance Adhesion, Cell Spread and Osteogenic Differentiation of Human Mesenchymal Stem Cells *in Vitro*. *Biomed. Mater.* **2007**, *2*, 116.
(27) Deligianni, D.; Korovessis, P.; Porte-Derrieu, M. C.; Amedee, J.; Repantis, T. Experimental Usage of Hydroxyapatite Preadsorption with Fibronectin to Increase Permanent Stability and Longevity of Spinal Implants. *Stud. Health Technol. Inf.* **2006**, *123*, 289.
(28) Mihailescu, I. N.; Ristoscu, C.; Bigi, A.; Mayer, I. Advanced Biomimetic Implants Based on Nanostructured Coatings Synthesized by Pulsed Laser Technologies. In *Laser-Surface Interactions for New Materials Production Tailoring Structure and Properties*; Miotello, A., Ossi, P. M., Ed.; Springer: New York, 2010; pp 235−260.
(29) Bigi, A.; Bracci, B.; Cuisinier, F.; Elkaim, R.; Fini, M.; Mayer, I.; Mihailescu, I.; Socol, G.; Sturba, L.; Torricelli, P. Human Osteoblast Response to Pulsed Laser Deposited Calcium Phosphate Coatings. *Biomaterials* **2005**, *26*, 2381−2389.
(30) Jansen, J. A.; Leon, B. *Thin calcium phosphate coatings for medical implants*; Springer: New York, 2009.
(31) Ribeiro, N.; Sousa, S. R.; Monteiro, F. J. Influence of Crystallite Size of Nanophased Hydroxyapatite on Fibronectin and Osteonectin Adsorption and on MC3T3-E1 Osteoblast Adhesion and Morphology. *J. Colloid Interface Sci.* **2010**, *351*, 398−406.
(32) Capuccini, C.; Torricelli, P.; Sima, F.; Boanini, E.; Ristoscu, C.; Bracci, B.; Socol, G.; Fini, M.; Mihailescu, I.; Bigi, A. Strontium-Substituted Hydroxyapatite Coatings Synthesized by Pulsed-Laser Deposition: *In Vitro* Osteoblast and Osteoclast Response. *Acta Biomater.* **2008**, *4*, 1885−1893.
(33) Ranella, A.; Barberoglou, M.; Bakogianni, S.; Fotakis, C.; Stratakis, E. Tuning Cell Adhesion by Controlling the Roughness and Wettability of 3D Micro/Nano Silicon Structures. *Acta Biomater.* **2010**, *6*, 2711−2720.
(34) Altankov, G.; Grinnell, F.; Groth, T. Studies on the Biocompatibility of Materials: Fibroblast Reorganization of Substratum-Bound Fibronectin on Surfaces Varying in Wettability. *J. Biomed. Mater. Res.* **1996**, *30*, 385−391.
(35) Groth, T.; Altankov, G. Studies on Cell-Biomaterial Interaction: Role of Tyrosine Phosphorylation during Fibroblast Spreading on Surfaces Varying in Wettability. *Biomaterials* **1996**, *17*, 1227−1234.
(36) Wei, J.; Igarashi, T.; Okumori, N.; Igarashi, T.; Maetani, T.; Liu, B.; Yoshinari, M. Influence of Surface Wettability on Competitive Protein Adsorption and Initial Attachment of Osteoblasts. *Biomed. Mater.* **2009**, *4*, 045002.
(37) Zhao, G.; Raines, A. L.; Wieland, M.; Schwartz, Z.; Boyan, B. D. Requirement for Both Micron- and Submicron Scale Structure for Synergistic Responses of Osteoblasts to Substrate Surface Energy and Topography. *Biomaterials* **2007**, *28*, 2821−2829.
(38) Linsley, C.; Wu, B.; Tawil, B. The Effect of Fibrinogen, Collagen Type I, and Fibronectin on Mesenchymal Stem Cell Growth and Differentiation into Osteoblasts. *Tissue Eng., Part A* **2013**, *19*, 1416−23.
(39) Yang, Y.; Glover, R.; Ong, J. L. Fibronectin Adsorption on Titanium Surfaces and Its Effect on Osteoblast Precursor Cell Attachment. *Colloids Surf., B* **2003**, *30* (4), 291−297.
(40) Pellenc, D.; Giraudier, S.; Champion, E.; Anselme, K.; Larreta-Garde, V.; Gallet, O. Removal of Surface By-products from Sintered Hydroxyapatite: Effect of a Chelation Treatment on Fibronectin Adsorption and Cell Adhesion. *J. Biomed. Mater. Res., Part B* **2006**, *76*, 136−142.
(41) Vohra, S.; Hennessy, K. M.; Sawyer, A. A.; Zhuo, Y.; Bellis, S. L. Comparison of Mesenchymal Stem Cell and Osteosarcoma Cell Adhesion to Hydroxyapatite. *J. Mater. Sci.: Mater. Med.* **2008**, *19*, 3567−3574.
(42) Pegueroles, M.; Aparicio, C.; Bosio, M.; Engel, E.; Gil, F. J.; Planell, J. A.; Altankov, G. Spatial Organization of Osteoblast Fibronectin Matrix on Titanium Surfaces: Effects of Roughness, Chemical Heterogeneity and Surface Energy. *Acta Biomater.* **2010**, *6*, 291−301.
(43) Bigi, A.; Nicoli-Aldini, N.; Bracci, B.; Zavan, B.; Boanini, E.; Sbaiz, F.; Panzavolta, S.; Zorzato, G.; Giardino, R.; Facchini, A.; Abatangelo, G.; Cortivo, R. *In Vitro* Culture of Mesenchymal Cells onto Nanocrystalline Hydroxyapatite-coated Ti13Nb13Zr Alloy. *J. Biomed. Mater. Res., Part A* **2007**, *82*, 213−21.
(44) Walsh, S.; Jordan, G. R.; Jefferiss, C.; Stewart, K.; Beresford, J. N. High Concentrations of Dexamethasone Suppress the Proliferation but not the Differentiation or Further Maturation of Human Osteoblast Precursors *in Vitro*: Relevance to Glucocorticoid-Induced Osteoporosis. *Rheumatology* **2001**, *40*, 74−83.
(45) Sima, L. E.; Stan, G. E.; Morosanu, C. O.; Melinescu, A.; Ianculescu, A.; Melinte, R.; Neamtu, J.; Petrescu, S. M. Differentiation of Mesenchymal Stem Cells onto Highly Adherent Radio Frequency-sputtered Carbonated Hydroxylapatite Thin Films. *J. Biomed. Mater. Res., Part A* **2010**, *95*, 1203−14.
(46) Costa, D. O.; Prowse, P. D. H.; Chrones, T.; Sims, S. M.; Hamilton, D. W.; Rizkalla, A. S.; Dixon, S. J. The Differential Regulation of Osteoblast and Osteoclast Activity by Surface Topography of Hydroxyapatite Coatings. *Biomaterials* **2013**, *34*, 7215−7226.
(47) Ripamonti, U.; Roden, L. C.; Renton, L. F. Osteoinductive Hydroxyapatite-Coated Titanium Implants. *Biomaterials* **2012**, *33*, 3813−3823.
(48) Hudalla, G. A.; Murphy, W. L. Biomaterials that Regulate Growth Factor Activity via Bioinspired Interactions. *Adv. Funct. Mater.* **2011**, *21*, 1754−1768.
(49) Zhang, J.-T.; Nie, J.; Mühlstädt, M.; Gallagher, H.; Pullig, O.; Jandt, K. D. Stable Extracellular Matrix Protein Patterns Guide the Orientation of Osteoblast-like Cells. *Adv. Funct. Mater.* **2011**, *21*, 4079−4087.
(50) Davies, J. E.; Ajami, E.; Moineddin, R.; Mendes, V. C. The Roles of Different Scale Ranges of Surface Implant Topography on the Stability of the Bone/Implant Interface. *Biomaterials* **2013**, *34*, 3535−3546.